Development of a probe based on UiO-66 MOF for determination of paclitaxel in urine samples

Reza Moharami [a,b] https://orcid.org/0009-0002-4395-1255 , **Zahra Karimzadeh** [c,d], **Yosra Vaez-Gharamaleki** [e], **Jafar Soleymani** [f], **Elaheh Rahimpour** [f,*] https://orcid.org/0000-0002-4037-9436 , **Abolghasem Jouyban** [f,g]

[a] Student Research Committee, Tabriz University of Medical Sciences, Tabriz, Iran
[b] Infectious and Tropical Diseases Research Center, Tabriz University of Medical Sciences, Tabriz, Iran
[c] Research Center for Pharmaceutical Nanotechnology, Biomedicine Institute, Tabriz University of Medical Sciences, Tabriz, Iran
[d] Engineered Biomaterials Research Center, Khazar University, Baku, Azerbaijan
[e] Hematology & Oncology Research Center, Tabriz University of Medical Sciences, Tabriz, Iran
[f] Pharmaceutical Analysis Research Center, Pharmaceutical Sciences Institute, Tabriz University of Medical Sciences, Tabriz, Iran
[g] Faculty of Pharmacy, Tabriz University of Medical Sciences, Tabriz, Iran

Submitted 2025/11/29
Revised 2026/4/11
Accepted 2026/4/15

Abstract

Introduction: Accurate and precise determination of paclitaxel is crucial due to its widespread use as a frontline treatment for various types of cancer, as well as its implementation in various drug delivery strategies. The objective of this study was to validate a facile fluorescent probe utilizing the UiO-66 metal-organic framework (MOF) to quantify paclitaxel in urine samples. **Results**: In the presence of paclitaxel and proportional to its concentration, the fluorescence intensity of UiO-66 MOF gradually decreased due to the formation a non-fluorescent complex during the interaction of paclitaxel and UiO-66 MOF. This platform demonstrated a linear response within the paclitaxel concentration range of 0.01 to 1.5 $\mu g.mL^{-1}$, with a detection limit of 0.007 $\mu g.mL^{-1}$. The UiO-66 MOF based probe's relative standard deviation for five replicated measurements of paclitaxel were 1.4% and 2.6% (n=5) for intra-day and inter-day, respectively. **Conclusion**: The results indicated that this robust and low-cost fluorescent probe was a promising platform for analyzing paclitaxel in clinical applications.

Keywords: UiO-66 MOFs; Fluorescent probe; Paclitaxel; Urine

Introduction

Paclitaxel is a compound with a tricyclic diterpenoid structure which can be found in the bark and needles of *Taxus brevifolia*.[1] In 1992, the Food and Drug Administration approved paclitaxel as a treatment for ovarian cancer. Since then, extensive research has been conducted on its efficacy in treating other cancers such as breast, prostate, bladder, cervical cancer and brain tumors. Additionally, it has been utilized to treat different medical conditions, including coronary heart disease, skin diseases, renal and hepatic fibrosis, and inflammation.[2] Paclitaxel is a pharmaceutical agent capable of disrupting the abnormal cell proliferation and mitosis rate in tumor cells. It accomplishes this by interacting with β-tubulin, a protein involved in the dynamic process, strengthening the lateral contacts between the subunits and stabilizing the microtubules.[3] It is considered one of the most important anti-cancer drugs used in therapeutic today.[4,5] Paclitaxel administration can cause different side effects, including peripheral neuropathy, nausea, hypersensitivity reactions, myelosuppression, myalgias, hypotension, bradycardia, arthralgias, diarrhea, mucositis, and alopecia.[6] Consequently, given the numerous side effects associated with paclitaxel, monitoring its concentration during treatment is essential. Many analytical techniques were used to determine paclitaxel in biological and environmental samples, such as reverse phase-high performance liquid chromatography (RP-HPLC),[7,8] micellar electrokinetic chromatography (MECK),[9] fluorescence immunoassay,[10] and electrochemical[11,12] procedures. These procedures require multiple pretreatment steps, costly laboratory equipment, or are time-consuming. Among them, fluorescent-based sensors offer easy operation and applicability in remote settings. However, these methods suffer from selectivity and sensitivity. To enhance the selectivity and sensitivity of fluorescent-based methods, the development of reliable platforms is necessary.[13] In this regard, metal-organic frameworks (MOFs) are a relatively new type of porous material made

from metal ions or clusters linked together by organic molecules. MOFs offer many advantages such as precise pore size, customizable composition and structure, adjustable size, adaptable functionality, high substance capacity, and enhanced biocompatibility.[14] Zirconium-based MOFs (Zr-MOFs) have high chemical and thermal stability due to strong coordination bonds between Zr and carboxyl groups of organic ligands.[15] While various types of MOFs are being researched and utilized by different groups, the UiO family, including UiO-66, UiO-67, and UiO-68, is the most commonly referenced.[16] UiO-66, a well-known member of the family of three-dimensional porous materials, comprises of Zr^{4+} and dicarboxylic acids.[17] Recent studies showed great interest in UiO-66 due to its structural durability and widespread popularity. Additionally, it exhibits remarkable characteristics such as a large surface area and uniform pore size, making it an exceptional choice in porous nanomaterials in sensing applications.[18] Despite various studies on UiO-66 MOF based systems for sensing applications, its utilization for monitoring anticancer drugs in biological fluids has been limited. This study examined the application of UiO-66 as a fluorescent probe for the direct, label-free detection of paclitaxel in urine samples. The proposed UiO-66-based platform provides a more straightforward, expedited, and cost-effective approach compared to conventional chromatographic or mass spectrometric methods. It necessitates no sample pretreatment or extraction procedures and preserves sufficient analytical sensitivity and selectivity for potential clinical application.[18]

Experimental Details

Materials

All analytical-grade chemicals were sourced commercially and utilized without further purification. Zirconium chloride ($ZrCl_4$, ≥99.5%), terephthalic acid, acetic acid (≥99.5%), and N,

N-dimethylformamide (DMF) were obtained from Sigma-Aldrich (USA) for the synthesis of UiO-66. A stock solution of paclitaxel (1000 $\mu g.mL^{-1}$) was kindly provided by Nanoalvand Pharmaceutical Company (Tehran, Iran) and diluted as required. Sodium hydroxide (NaOH) and hydrochloric acid (HCl), both obtained from Merck (Germany) were used for pH adjustment. Ultrapure deionized water was obtained from Shahid Ghazi Pharmaceutical Co. (Tabriz, Iran) for dilution.

Instruments

Fluorescence spectra were measured using a Jasco Corp. FP-750 spectrofluorometer (Japan), equipped with a xenon lamp source, with bandwidths adjusted at 10 nm for excitation and 5 nm for emission pathways. A 1 mL standard quartz cell was employed for recording all fluorescence spectra. UV-vis absorption spectra of the prepared solutions were recorded on a Shimadzu model UV-1800 spectrophotometer (Japan) using a micro quartz cell. The size distribution of the prepared probe was determined and evaluated using a Philips CM30 transmission electron microscopy (TEM) (Netherlands). For investigating the crystallite, Powder X-ray diffraction (XRD) was accomplished using a Siemens diffractometer at 35 kV within the 2θ range of 4–70°. The Brunauer-Emmett-Teller (BET) surface area was analyzed using the BEL-SORP MINI II (Japan) via the N_2 adsorption method. Fourier transforms infrared (FT-IR) spectroscopy was accomplished on Bruker Tensor 270 to verify the chemical bindings. Additionally, the synthesis of UiO-66 was conducted in an Initiator 8 EXP oven (Biotage Corp.) at a frequency of 2450 MHz. pH adjustments were performed using a Metrohm Ltd. model 744 digital pH meter (Switzerland).

Synthesis of UiO-66 MOF

UiO-66 MOF was synthesized using a previously reported method, using terephthalic acid and $ZrCl_4$ as reactants.[19] To prepare the nanomaterial, a solution was first prepared by separately

dissolving 40.8 mg of $ZrCl_4$ in 5 mL of DMF and 26.6 mg of terephthalic acid in 5 mL of DMF at room temperature. Next, 0.5 mL of stock acetic acid (≥99.5%) was added to the mixture, which was then transferred to a Teflon-lined autoclave and heated at 120 °C without stirring for 24 hours. After this treatment, the UiO-66 product was isolated through centrifugation and washed multiple times with DMF and methanol. Finally, the resulting solid was dried overnight under vacuum at 60 °C for further use in the experiments.

Samples preparation

Urine samples were collected from patients who received a dose of 100 mg paclitaxel. The urine samples were obtained by collecting 24-hour samples in dark glass bottles. Except for a 10-fold dilution with distilled water, no further processing was necessary before analysis. The urine samples were diluted 10-fold with distilled water prior to analysis to minimize potential matrix effects arising from proteins, electrolytes, and other endogenous compounds, which could interfere with fluorescence measurements. Preliminary optimization experiments indicated that this dilution factor provided a stable fluorescence signal. Informed consent was obtained from the sample donors, approved by the Ethics Committee of Tabriz University of Medical Sciences with the approved code of IR.TBZMED.REC.1402.601.

General procedure

An optimized condition was employed to prepare the sample mixture by combining 20 µL of 0.1 mol L^{-1} acetate buffer (pH 5.0) with 100 µL of diluted human urine in a microtube. Subsequently, 20 µL of UiO-66 MOF (1000 $mg.L^{-1}$) was added, followed by deionized water to a final volume of 0.5 mL. The mixture was incubated for 10 minutes at room temperature before fluorescence measurement at λ_{ex} = 280 nm and λ_{em} = 417 nm. The analytical response was quantified as ΔF (F_0-

F), where *F* represents the fluorescence intensity in the presence of paclitaxel and F_0 represents the fluorescence intensity in its absence. The protocol was repeated three times under identical conditions at room temperature.

Results and discussions

Characterization of synthesized UiO-66 MOF

TEM is a microscopy technique in which a beam of electrons is transmitted through a specimen to form an image. It was utilized to characterize the particle size and morphology of UiO-66 MOF (Figure 1A). Based on the results, UiO-66 nanoparticles were tetrahedral and octahedral cage with an average particle size of lower than 200 nm.

The structural properties of UiO-66 were further confirmed by XRD analysis. Characteristic peaks for UiO-66 MOF appeared at 2θ = 7.3°, 8.5°, and 25.7°, corresponding to the (111), (002), and (006) planes, respectively. This confirmed the successful synthesis and high crystallinity of the material. These diffraction peaks were consistent with the simulated pattern and previous reports for UiO-66, indicating that the framework structure was well preserved during synthesis. To characterize the surface area of UiO-66, the N_2 adsorption-desorption analysis was used at 77 K (Figure 1B). This method is widely used to measure the specific surface area and pore size distribution of materials. The UiO-66 exhibited a type I adsorption isotherm, with no observable hysteresis. At elevated pressures, the curve may be attributed to the imprecise measurement of available space. The BET surface area of UiO-66 was 1208 $m^2 g^{-1}$.

To show the successful synthesis of UiO-66 and the interaction of UiO-66 with paclitaxel, FT-IR spectrum was performed. The absorption band at around 1393 and 1565 cm^{-1} in UiO-66 could be related to the stretching vibration of the terephthalic acid's carboxylate groups. Additionally, the intense aromatic/benzene ring vibrations in UiO-66 were displayed around 1600 cm^{-1}. After the

addition of paclitaxel, its peaks were overlapped with MOF linker vibrations in the 1300–1000 cm^{-1} regions. This produced broadened and blended features in the composite. The slight perturbation (shift and intensity change) of the UiO-66/paclitaxel were consistent with hydrogen bonding and/or polar interactions between paclitaxel functional groups (especially OH and C=O groups) and the MOF pore surface, and with confinement effects inside the pores, suggesting non-covalent interactions. Importantly, the retention of the Zr–O stretching modes in the ~650–500 cm^{-1} region confirmed that the UiO-66 framework remained intact. Furthermore, the appearance of the ester/carbonyl bands of paclitaxel and a shift of the O-H stretching region, and carboxylate bands of the MOF were consistent with physical adsorption of paclitaxel inside UiO-66 via hydrogen bonding and van der Waals/π–π interactions rather than formation of new covalent bonds.

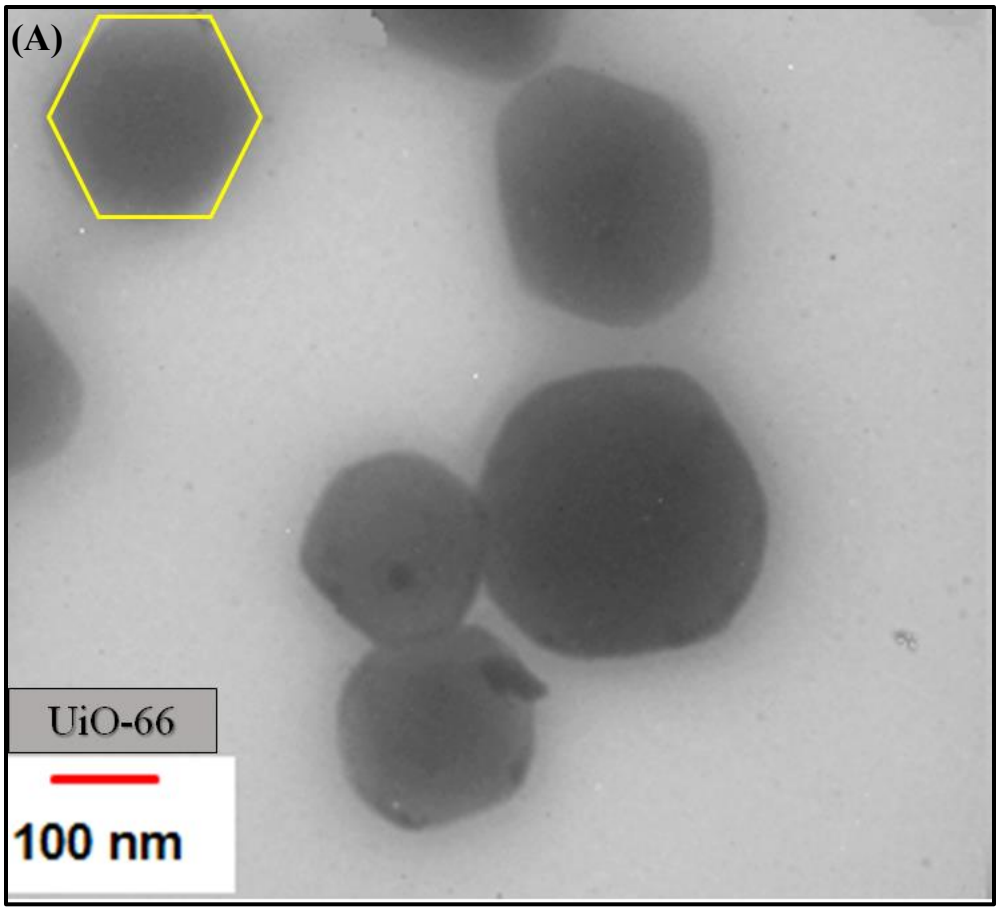

Fig. 1A

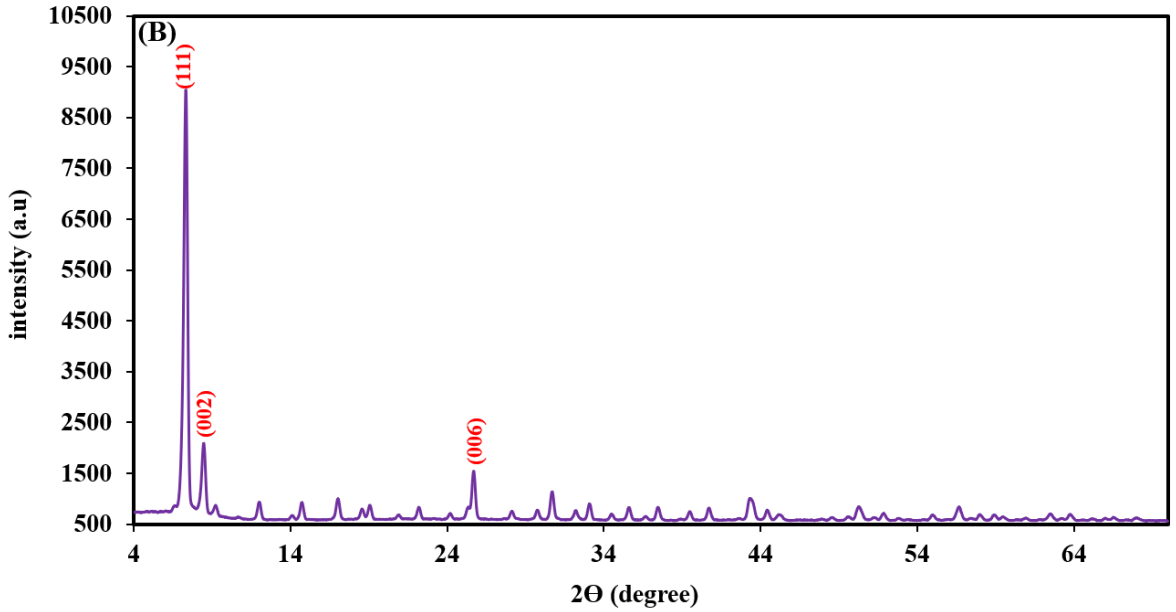
(B)
(111)
(002)
(006)
intensity (a.u)
10500
9500
8500
7500
6500
5500
4500
3500
2500
1500
500
4
14
24
34
44
54
64
2Θ (degree)

Fig. 1B

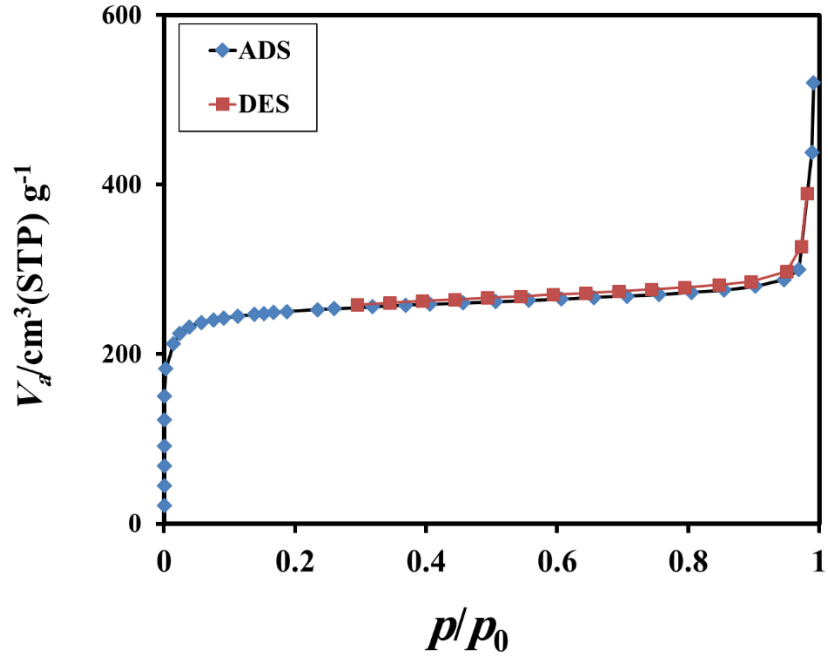
ADS
DES
600
400
200
0
0
0.2
0.4
0.6
0.8
1
V_d/cm^3(STP) g^{-1}
p/p_0

Fig. 1C

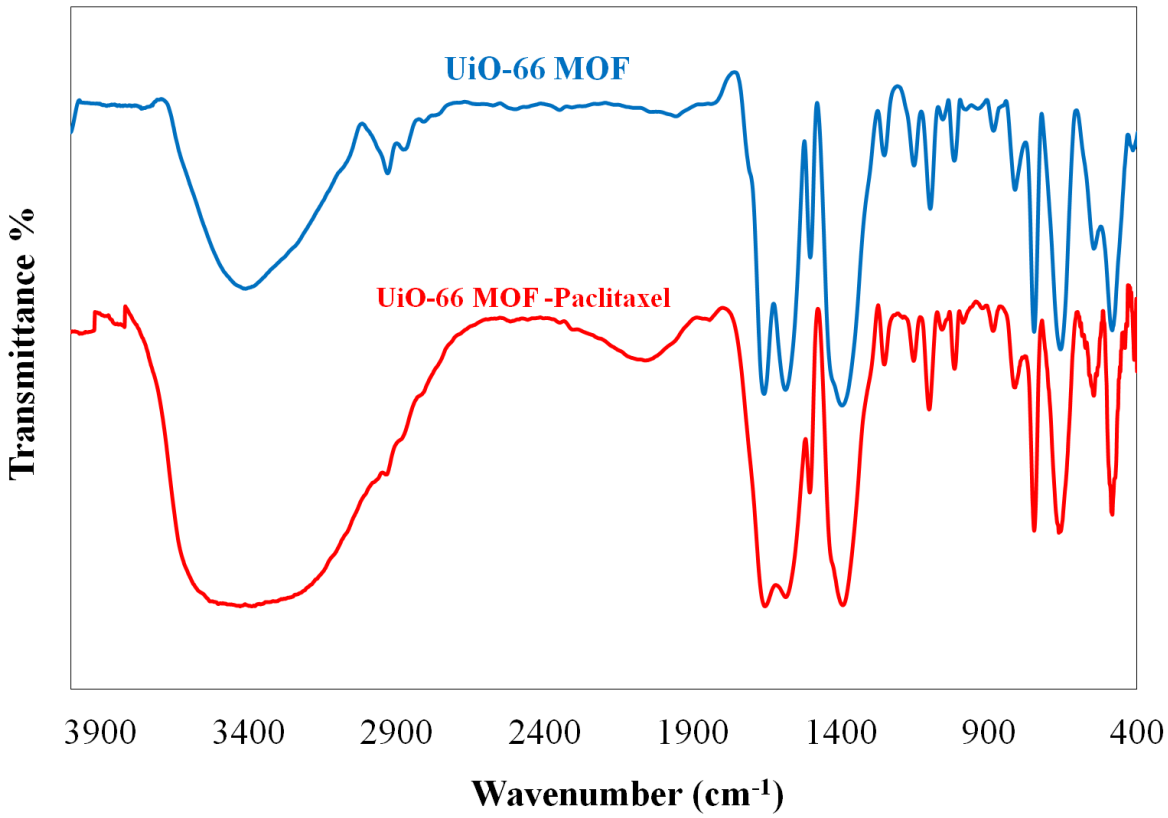

Fig. 1D

Figure 1. (A) TEM images, **(B)** XRD analysis and, **(C)** N_2 adsorption–desorption isotherms at 77 K of UiO-66 and **(D)** FT-IR spectra of UiO-66 in the absence and presence of paclitaxel

Sensing mechanism

Zr-based UiO-66 is characterized by its structural composition of zirconium clusters interconnected by terephthalic acid ligands, which exhibit fluorescence owing to the π-conjugated system of the ligands and the zirconium coordination environment.[16] The analysis revealed a characteristic emission peak at 417 nm for UiO-66. Upon adding paclitaxel, the fluorescence intensity of the UiO-66 MOF based probe decreased significantly, suggesting a specific interaction between paclitaxel and the UiO-66. Paclitaxel interacts with UiO-66 through a combination of four interactions of (i) hydrogen bonding, (ii) π-π stacking, (iii) coordination to metal centers, and (iv)

electrostatic interactions. The hydroxyl group and carbonyl group on paclitaxel can form hydrogen bonds with the carboxyl groups on the terephthalic acid ligand.[20] They can be coordinated to the Zr centers in UiO-66, forming a coordination complex,[21] while the planar aromatic rings on paclitaxel interact with the planar aromatic rings on the terephthalic acid ligands through π-π stacking.[22] The positively charged amine groups on paclitaxel also interacted with the negatively charged carboxyl groups on the terephthalic acid ligands, leading to electrostatic attraction.[23] This interaction resulted in the formation of a non-fluorescent complex, accompanied by a corresponding reduction in the fluorescence intensity of the UiO-66. The observed decrease in fluorescence intensity was directly proportional to the amount of paclitaxel present, indicating a promising approach for quantitatively monitoring paclitaxel concentrations in urine samples.

The mechanism of fluorescence quenching was checked through Stern-Volmer plots, which involved plotting the fluorescence intensity ratio (F_0/F) against the concentration of the quencher, according to the below equation.

$$\frac{F_0}{F} = 1 + K_{sv}[Q] \quad (1)$$

Where F_0 and F represent the fluorescence intensity in the absence and presence of the quencher, respectively, K_{SV} is the Stern-Volmer constant, and $[Q]$ is the quencher concentration. Stern-Volmer plots can display both static and dynamic quenching modes.[24] A linear Stern-Volmer plot shows a dynamic quenching, which the quencher primarily enhances collisional interactions with the fluorophore, leads to efficient energy transfer. Conversely, an upward or positive deviation in the Stern-Volmer plot may suggest the involvement of both static and dynamic quenching mechanisms, which together lead to a reduction in fluorescence intensity. The upward trend observed in Figure 2 confirmed the presence of static quenching or the formation of a complex

between the fluorophore and quencher, implying the existence of a non-fluorescent ground-state complex.

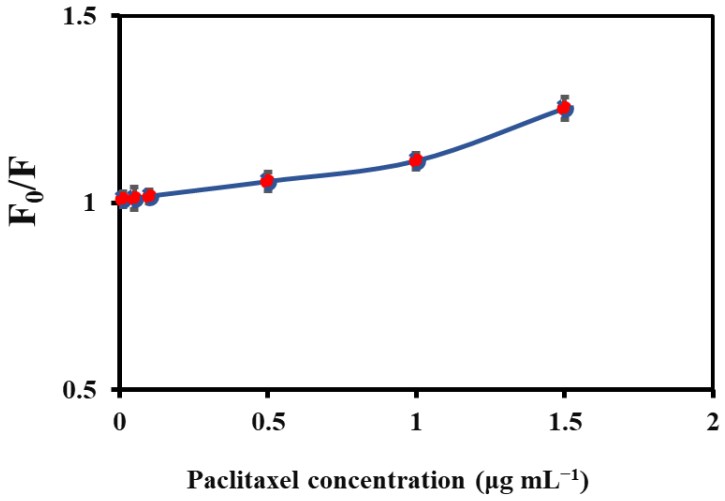

Figure 2. Stern–Volmer plot for the quenching of UiO-66 MOF based probe by paclitaxel. Condition: pH: 5.0, UiO-66 amount: 20 µL of stock solution 1000 mg.L^{-1}, incubation time: 10 min, and room temperature (λ_{ex} = 340 nm, λ_{em} = 417 nm).

Optimization studies

The importance of experimental conditions for probe response is paramount, as they directly affect probe performance. Preliminary experiments indicated that the fluorescent intensity was affected by four factors: pH, UiO-66 MOF volume, incubation time, and temperature. Paclitaxel in a concentration of 1.0 µg.mL^{-1} was used in the optimization procedure. This study used buffer (0.10 mol.L^{-1}) to investigate the effect of pH values ranging from 3.0 to 11.0 on the fluorescence response. The highest ΔF was obtained at pH 5.0, which was identified as the optimum pH value as illustrated in Figure 3A. This can be related to the interaction of the positively charged amine groups on paclitaxel (pK_a=10.9) with the negatively charged groups on the terephthalic acid

ligands (pK_a=4.34). In the following, different volumes of UiO-66 MOF (1000 mg.L^{-1}) were utilized to determine the optimal amount of UiO-66 MOF during the design process. The result indicated that the highest response of the UiO-66 MOF based probe was obtained at 20.0 µL of UiO-66 MOF (1000 mg.L^{-1}) and more than this amount, a decrease in response was observed due to nanoparticle self-quenching in high concentration (Figure 3B). The time taken for the reaction of paclitaxel molecules and UiO-66 MOFs-based probe and reaching equilibrium is called the incubation time. The incubation time for this reaction was examined over various durations ranging from immediately analysis up to 20 min. As shown in Figure 3C, the response of the probe reached a maximum of 10 min. So, 10 min was selected as the optimal incubation time for the following experiments. It should be mentioned that temperature, another factor influencing fluorescence response, was also examined in the 5–45 °C range. The optimal reaction was observed between 5 and 30 °C. So, the experiments were performed at room temperature.

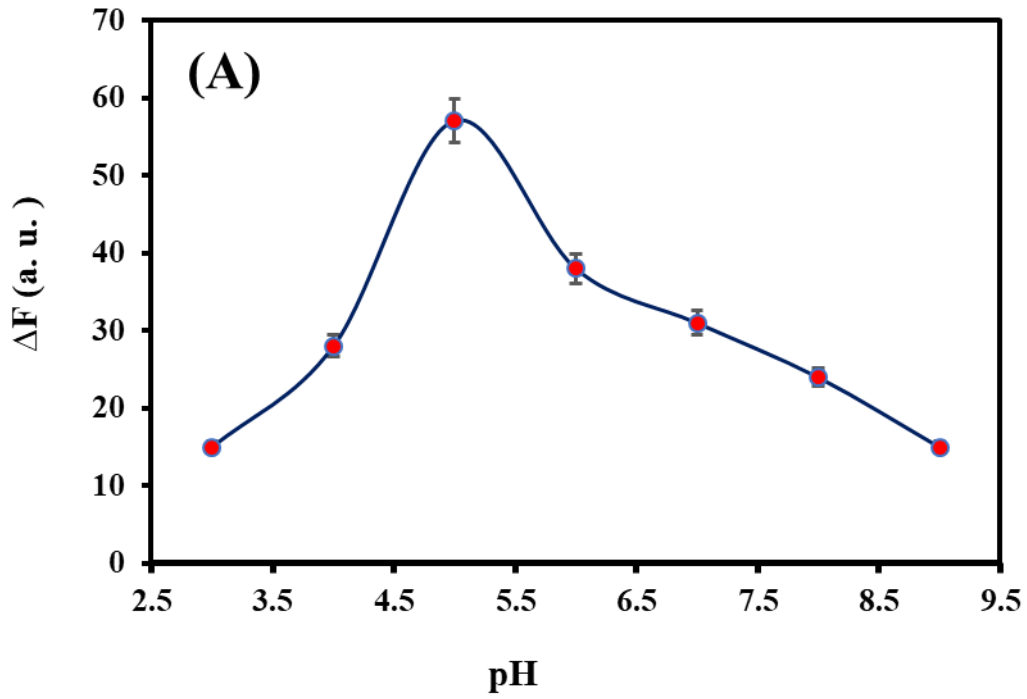

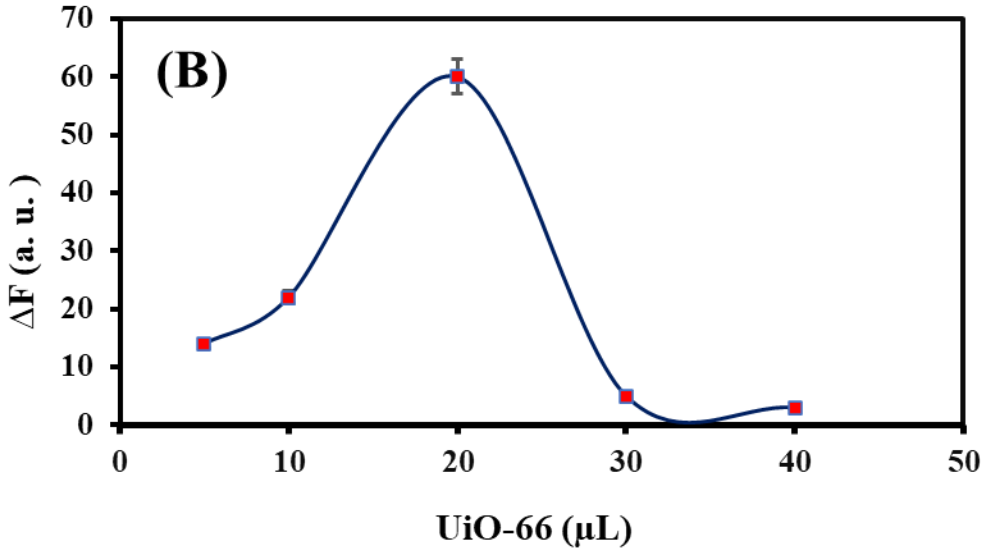
(B)
ΔF (a. u.)
UiO-66 (μL)
0
10
20
30
40
50
60
70

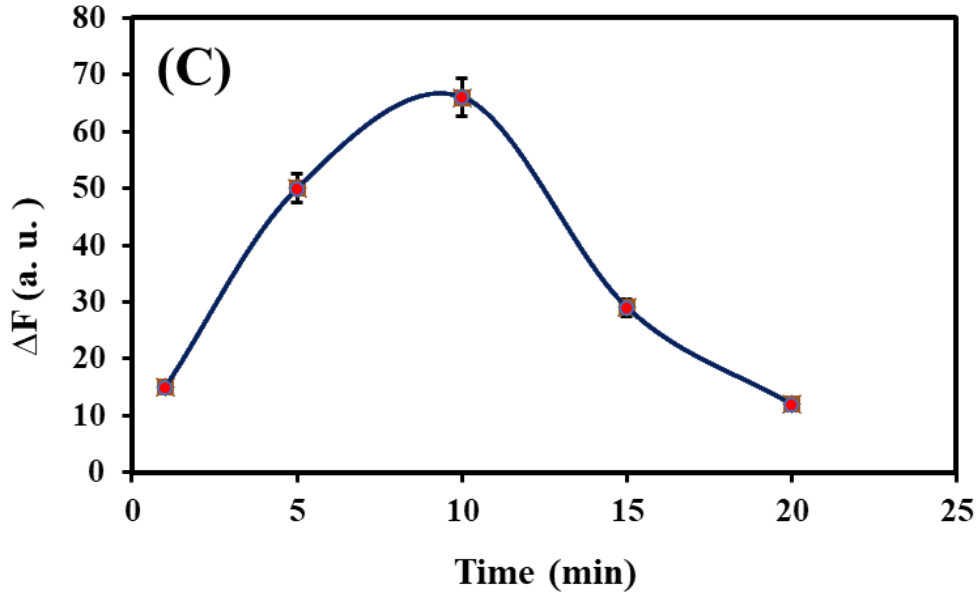
(C)
ΔF (a. u.)
Time (min)
0
5
10
15
20
25
10
20
30
40
50
60
70
80

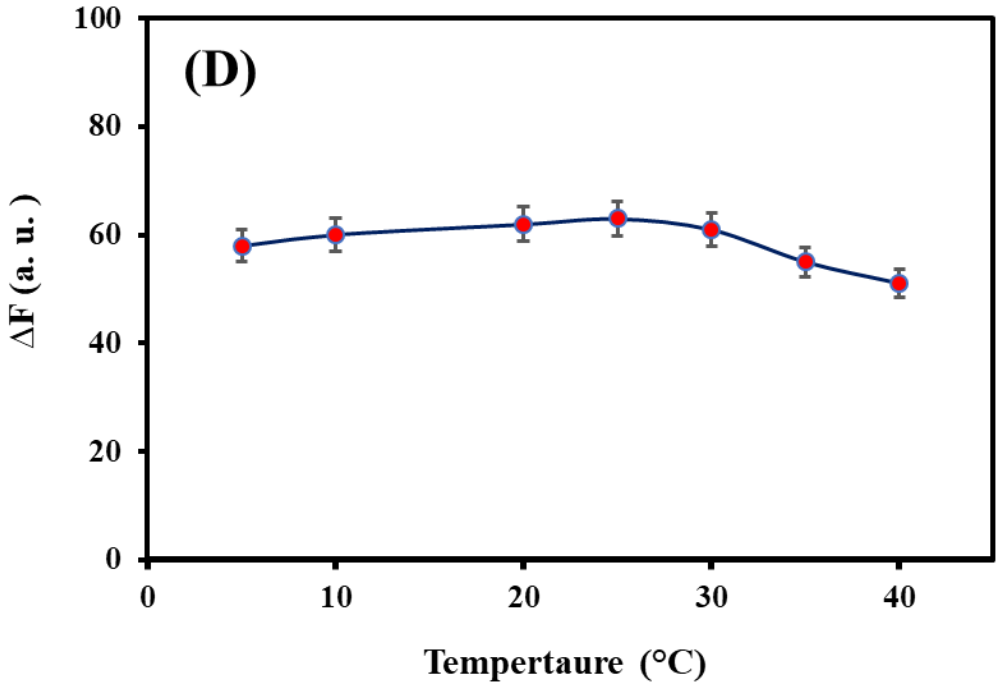

Figure 3. Effect of **(A)** pH, **(B)** UiO-66 amount, **(C)** incubation time, and **(D)** temperature on the fluorescence response of the UiO-66 probe toward paclitaxel (1.0 μg.mL^{-1}) (λ_{ex} = 340 nm, λ_{em} = 417 nm). Error bars represent standard deviation for n = 3.

Analytical figures of merit

To evaluate the response of the UiO-66 MOF based probe to paclitaxel, the concentration-dependent behavior of the method was studied under optimal conditions. As shown in Figure 4, an increase in paclitaxel concentration led to a gradual decrease in fluorescence intensity of UiO-66 MOF-based probe at around 417 nm. Based on the results, there was a respectable linear relationship between the fluorescence intensity and paclitaxel concentration in the range of 0.01–1.5 μg.mL^{-1} as shown in Figure 4. The regression equation was $\Delta F = 50.95\ C_{PTX} + 5.8328$ (R_2 = 0.9919) where C_{PTX} represented the concentration of paclitaxel in μg.mL^{-1}, F_0 and F indicated the fluorescence intensity in the absence and presence of paclitaxel at 417 nm, respectively. The limit of detection (LOD) and limit of quantification (LOQ) were calculated based on $3S_b/m$ (S_b: blank's

standard deviation; m: calibration slope) and 10 S_b/m, and were found to be 0.007 and 0.024 $\mu g.mL^{-1}$, respectively. To study the precision of the procedure, the paclitaxel analysis was repeated during the same and different days. The intra-day and inter-day relative standard deviations (*RSDs* %) for five replicate determinations of paclitaxel (1.0 $\mu g.mL^{-1}$) were found to be 1.4% and 2.6%, respectively. The validated process demonstrated improved repeatability and reproducibility, indicating that the proposed UiO-66 MOF-based probe could be effective for determining paclitaxel. Table 1 provided a summary of the analytical characterization of the validated method for paclitaxel determination, comparing it to other methods reported in the literature. The results indicated that the LOD and linear range of this method were similar to those reported by other researchers. While this method's performance was on par with existing methods, its unique advantage lies in its simplicity and rapidity, as it allows for direct measurement without the need for sample preparation before analysis. In contrast, most existing methods for paclitaxel determination required liquid or solid-phase extraction for cleanup and analyte preconcentration. The results indicated that the proposed probe performed well for paclitaxel determination. However, there are challenges associated with the probe that limit its application. This is poor storage stability of the UiO-66 MOF based probe over extended periods due to nanomaterial nature and large surface area, which can lead to particle aggregation and complicate handling in liquid form. In this work, stability studies were also conducted, and as you can see in Figure 5, the intensity of the synthesized probe remained stable for about a month, after which it gradually decreased. The observed decrease in fluorescence intensity after prolonged storage was likely due to partial aggregation of UiO-66 nanoparticles and minor framework degradation under aqueous conditions. The stability of the probe can be improved by storing UiO-66 in dry form and freshly re-dispersing it before use, or by introducing surface modifiers such as poly(vinylpyrrolidone) or

polyethylene glycol to reduce aggregation. In addition, post-synthetic functionalization of UiO-66 with hydrophilic ligands or carboxylate groups may further enhance its hydrolytic stability, thereby extending its shelf-life for the practical applications.

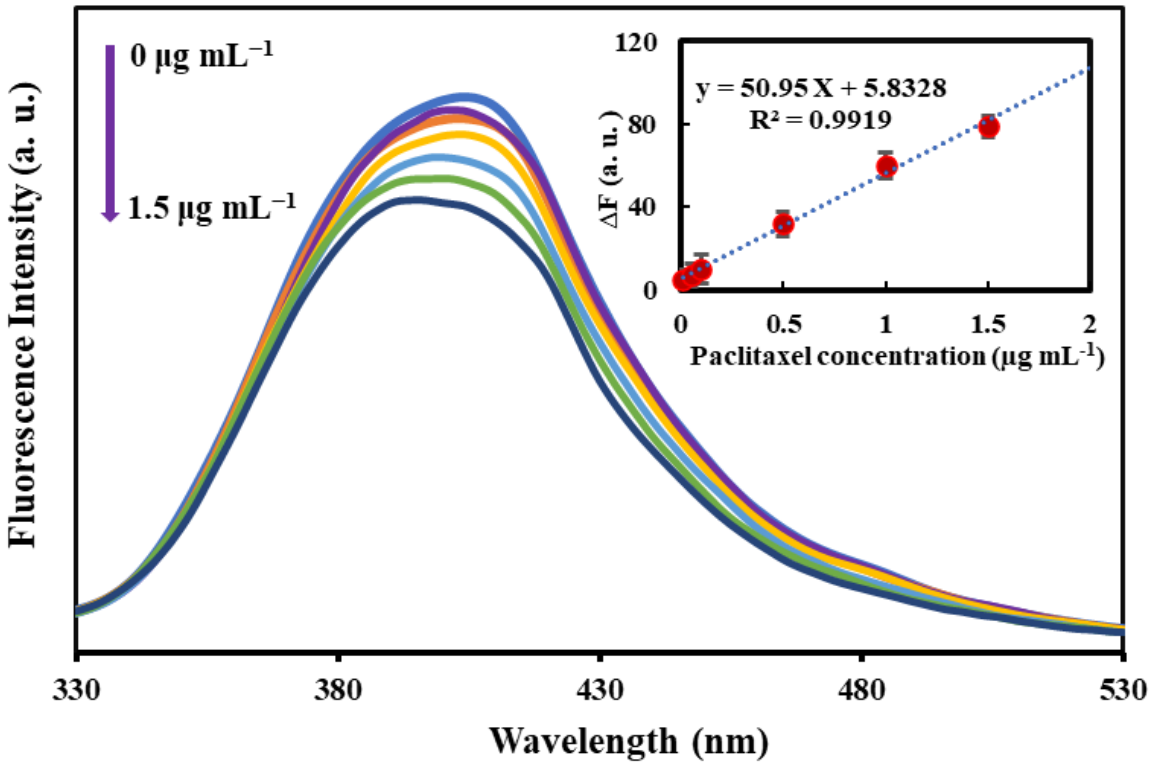

Figure 4. Fluorescence intensity of probe based on UiO-66 MOF in the absence and presence of paclitaxel in the range of 0.01–1.5 µg.mL^{-1}, Condition: pH: 5.0, UiO-66 amount: 20 µL, incubation time: 10 min, and room temperature (λ_{ex} = 340 nm, λ_{em} = 417 nm).

Table 1

Comparison of analytical characteristics of this method with published methods for the determination of paclitaxel

Method	Sample	LOD (µg.mL^{-1})	Linear range (µg.mL^{-1})	Reference
Voltammetry	Urine	0.010	0.85 - 8.53	[25]

Luminol@ carbon nanotubes and CdTe-ZnS@ hydroxyapatite based electrochemiluminescence sensor	Serum	8.5×10^{-7}	2.6×10^{-6} – 0.2	[26]
Carbon dots based electrochemical method	Serum Urine	1.7×10^{-3}	5.9×10^{-2} - 30	[27]
Gold-based multiplex immunochromatographic sensor	Plasma Urine	-	0.002 -0.142	[28]
HPLC-UV[a]	Pharmaceutical dosage form	0.001	0.005 – 50.0	[29]
LC–MS/MS[b]	Taxus species	0.008	0.060–38.8	[30]
MEKC	Serum	0.09	0.28–50.0	[31]
Immunoassay	Plasma	0.011	0.019-0.320	[32]
Porous molecularly imprinted polymer-ZnS quantum dots based - Spectrophotometry	Plasma	36.71	85.39-1,707.80	[33]
icELISA[c]	Yew tree	0.0098	0.098-312.5	[34]
UiO-66 MOF based fluorescence assay	Urine	0.007	0.01-1.5	This work

[a] High-performance liquid chromatography- Ultraviolet, [b] Liquid Chromatography-Tandem mass spectroscopy, [c] Micellar electrokinetic chromatography, [c] indirect competitive enzyme-linked immunosorbent assay

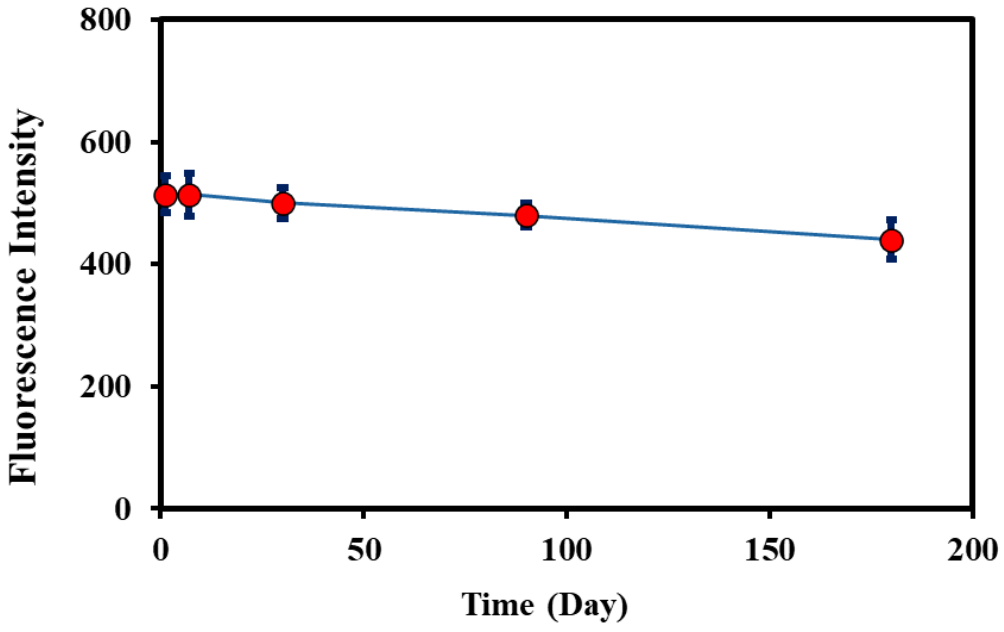

Figure 5. Stability study of the UiO-66-based probe intensity under optimized conditions

Interference study

To evaluate the method selectivity, the response of the UiO-66 MOF-based probe to potential co-administrated and over-the-counter drugs was studied. The available interfering substances included oxazepam, losartan, dexamethasone, diazepam, pantoprazole, ampicillin, uric acid, alprazolam, diltiazem, amoxicillin, chlordiazepoxide, cetirizine, and clonazepam. The response of the probe was measured at a concentration of 1.0 $\mu g.mL^{-1}$ for paclitaxel and all interfering substances with the same concentration were spiked in the distinct micro-tubes containing urine, pH 5.0, and 20.0 µL of UiO-66 MOF. As shown in Figure 6, the addition of interferences to the probe had a negligible effect on the fluorescence response of the probe, indicating the system has good selectivity and sensitivity for determining paclitaxel in urine samples.

It should be noted that the drugs examined in the interference section of this study are available compounds in our laboratory. If someone wants to extend the method to other biological matrices, they must investigate other interfering substances and drugs relevant to that matrix. It may be necessary to use preparation or separation methods to address these interferences.

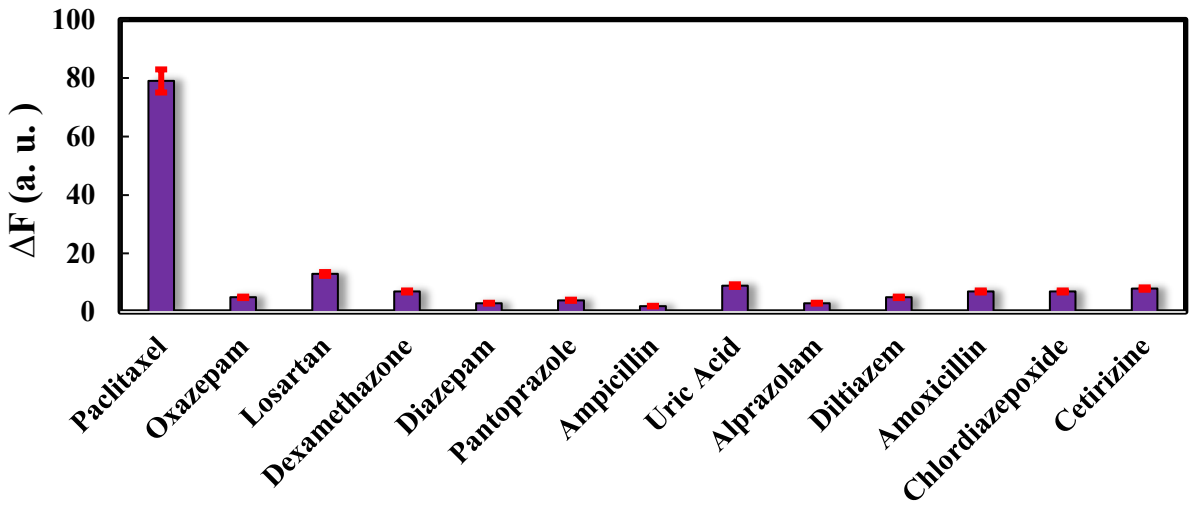

Figure 6 Interference study on probe response. The concentrations of all drugs were 1.0 μg.mL^{-1}

Furthermore, the impact of some interfering organic substances and inorganic ions normally existing in the urine was also studied on the paclitaxel determination and results was given in Table 2. The response of the probe was measured at a concentration of 1.0 μg.mL^{-1} for all interfering substances in the presence of 1.0 μg.mL^{-1} paclitaxel. Low variation ($\Delta F < \pm 10$) in the probe response, proved that the validated method has good selectivity for paclitaxel analysis in urine samples.

Table 2
Effect of interfering substances normally exist in the urine media on the paclitaxel analysis

Interfering species	***ΔF***
Glucose	-1
Uric acid	-9
HPO_4^{2-}	-3
Cl^-	-7
SO_4^{2-}	-7
K^+	-3
NH_4^+	-10
Na^+	-4
Ca^{2+}	-8
Mg^{2+}	+5

Real samples analysis

The proposed UiO-66 MOF-based probe was utilized to quantify paclitaxel in four urine samples obtained from female patients who received paclitaxel treatment. The results of the real sample analysis were presented in Table 3. To validate the accuracy of the reported values and investigate potential interference from co-administered drugs, recovery experiments were conducted by spiking each urine sample with 1.0 $\mu g.mL^{-1}$ of standard paclitaxel solution. The results demonstrated a satisfactory recovery range of 90.0-103.3%, indicating high accuracy and minimal matrix effects for determining paclitaxel in complex biological matrices such as urine. It should be noted that there was no gender bias in the application of this method. The reason for analyzing paclitaxel only in female samples was that the volunteers who provided samples were these women. It should be noted that the number of analyzed samples in this study was limited due to the availability of patient volunteers undergoing paclitaxel therapy and the ethical approval constraints associated with clinical sample collection. Therefore, this work should be regarded as a preliminary feasibility study demonstrating the analytical performance of the UiO-66-based probe. Future investigations will focus on analyzing a larger and more diverse patient population, including both male and female subjects.

Additionally, samples 1 and 2 were also analyzed using HPLC-UV as a standard method. The concentrations of paclitaxel in patient samples 1 and 2 were found to be 0.079 ± 0.008 and 0.15 ± 0.011 $\mu g.mL^{-1}$, respectively. The statistical analysis of these results with those obtained from the validated method (0.08 ± 0.008 and 0.16 ± 0.012 $\mu g.mL^{-1}$ for samples 1 and 2, respectively) was confirmed through a paired *t*-test (2-tailed), indicating no significant difference between the results at a 95% confidence

level. These findings suggested that the proposed method has strong potential for determining paclitaxel levels in the investigated biological samples.

Table 3. Determination of paclitaxel in real urine samples by validated UiO-66 MOF-based probe.

No.	Gender	Age (year)	Co-administrated drugs	Added ($\mu g.mL^{-1}$)	Found ($\mu g.mL^{-1}$)	Recovery (%)[a]
1	Female	53	_	-	0.08	-
				0.1	0.18	100.0
				0.6	0.69	101.7
2	Female	38	Doxorubicin, Cyclophosphamide	-	0.16	-
				0.1	0.25	90.0
				0.6	0.77	101.7
3	Female	50	Doxorubicin, Cyclophosphamide	-	0.12	-
				0.1	0.22	100.0
				0.6	0.74	103.3
4	Female	42	Cyclophosphamide, Doxorubicin, Granisetron, Pegfilgrastim	-	0.10	-
				0.1	0.20	100.0
				0.6	0.72	103.3

[a] Recovery (%) = [paclitaxel concentration in samples (after spiking – before spiking)/Added] × 100.

Conclusion

In summary, a fluorescent UiO-66 MOF-based probe has been designed based on UiO-66 MOF for the quantitatively detection of paclitaxel. The addition of paclitaxel resulted in a decrease in the probe's fluorescent intensity, creating a system for concentration-dependent sensing of paclitaxel in urine samples. This probe revealed a linear response for paclitaxel in a broad range of 0.01-1.5 $\mu g.mL^{-1}$ with low LOD of 0.007 $\mu g.mL^{-1}$ and high selectivity. The validated method was successfully employed for the determination of paclitaxel in the urine samples of patients receiving this medication with high recovery in the range of 90.0%–103.3%. This study may provide a promising probe for rapidly, sensitively, and selectively detecting paclitaxel in urine samples. In modest experimental conditions, this study demonstrated that employing UiO-66 as a

fluorescent probe for the direct detection of paclitaxel in urine is viable. While analogous methods have been utilized in several sensing contexts, therapeutic drug monitoring has not garnered equivalent focus. The proposed method offered advantageous features compared to conventional HPLC and LC–MS/MS techniques, including ease of operation, cost-effectiveness, and rapid analysis. However, it should be noted that this study has limitations due to a small and diverse sample size and reliance on fluorescence quenching, which affects generalizability and sensitivity. We suggested that future research can be focused on enhancing probe stability, broadening sample diversity, and investigating applications in other biological matrices. Furthermore, extending the investigation to other hydrophobic MOF systems (*e.g.,* UiO-67, MIL-101(Cr)) could further validate and optimize the sensing performance.

Ethical approval and consent to participate

All sample donors or participants filled out and signed the informed consent of project with ethical code IR.TBZMED.REC.1402.601 confirmed by the ethics committee at Tabriz University of Medical Sciences verified.

Funding statement

The research protocol was approved and supported by the Student Research Committee under grant number 72309, Faculty of Pharmacy, Tabriz University of Medical Sciences, Tabriz, Iran.

Data availability statement

Data supporting this study are included within the article

Authorship contribution statement

Conceptualization: **Abolghasem Jouyban**

Data curation: **Zahra Karimzadeh**

Formal analysis: **Zahra Karimzadeh**

Funding acquisition: **Reza Moharami**

Investigation: **Reza Moharami**

Methodology: **Elaheh Rahimpour**

Project administration: **Elaheh Rahimpour**

Resources: **Yosra Vaez-Gharamaleki**

Software:-

Supervision: **Elaheh Rahimpour, Abolghasem Jouyban**

Validation: **Jafar Soleymani**

Visualization: **Jafar Soleymani**

Writing–original draft: **Zahra Karimzadeh**

Writing–review & editing: **Elaheh Rahimpour, Abolghasem Jouyban**

Declaration of competing interest

The authors declare that they have no known competing financial interests or personal relationships that could have appeared to influence the work reported in this paper.

Acknowledgements

None.

References

1. Zhu L, Chen LJC. Progress in research on paclitaxel and tumor immunotherapy, Cell. Mol. Biol. Lett. 2019;24:40. https://doi.org/10.1186/s11658-019-0164-y.

2. Zhang D, Yang R, Wang S, Dong Z. Paclitaxel: new uses for an old drug, Drug Des. Devel. Ther. 2014;8:279–84. https://doi.org/10.2147/DDDT.S56801

3. Klein I, Lehmann HC, Pathomechanisms of paclitaxel-induced peripheral neuropathy, Toxics 2021;9:229. https://doi.org/10.3390/toxics9100229.

4. Bernabeu E, Cagel M, Lagomarsino E, Moretton M, Chiappetta DA. Paclitaxel: what has been done and the challenges remain ahead, Int. J. Pharm. 2017;526:474–95. https://doi.org/10.1016/j.ijpharm.2017.05.016.

5. Mollaei H, Babaei E, Therapeutic potential of novel nano-based curcumin compounds in vitro and in vivo, Asian Pac. J. Cancer Prev. 2017;18: 885–8. https://doi.org/10.22034/APJCP.2017.18.4.885.

6. Marupudi NI, Han JE, Li KW, Renard VM, Tyler BM, Brem HI. Paclitaxel: a review of adverse toxicities and novel delivery strategies, Expert Opin. Drug Saf. 2007;6: 609–21. https://doi.org/10.1517/14740338.6.5.609.

7. Kumar G, Mullick P, Nandakumar K, Mutalik S, Rao CM. Box–Behnken design-based development and validation of a reverse-phase HPLC analytical method for the estimation of paclitaxel in cationic liposomes, Chromatographia 2022;85:247–54. https://doi.org/10.1007/s10337-022-04128-0.

8. Yadav A, Pandey S, Mandal MK, Dubey KK. Development of cost-effective RP-HPLC methods for detection of cyclophosphamide, etoposide and paclitaxel, Sep. Sci. Plus 2020;3:40–3. https://doi.org/10.1002/sscp.201900071.

9. Rodríguez J, Castañeda G, Contento AM, Muñoz L. Direct and fast determination of paclitaxel, morphine and codeine in urine by micellar electrokinetic chromatography, J. Chromatogr. A 2012;1231:66–72. https://doi.org/10.1016/j.chroma.2012.02.003.

10. Sheikh SH, Abela BA, Mulchandani A. Development of a fluorescence immunoassay for measurement of paclitaxel in human plasma, Anal. Biochem. 2000;283;33–8. https://doi.org/10.1006/abio.2000.4630.

11. Lang J, Wang W, Zhou Y, Guo D, Shi R, Zhou N. Electrochemical behavior and direct quantitative determination of paclitaxel, Front. Chem. 2022;10: 834154. https://doi.org/10.3389/fchem.2022.834154.

12. Gowda JI, Nandibewoor ST. Electrochemical characterization and determination of paclitaxel drug using graphite pencil electrode, Electrochim. Acta 2014;116: 326–33. https://doi.org/10.1016/j.electacta.2013.11.014.

13. Gao M, Tang BZ. Fluorescent sensors based on aggregation-induced emission: recent advances and perspectives, ACS Sens. 2017:2: 1382–99. https://doi.org/10.1021/acssensors.7b00551.

14. Cao J, Li X, Tian H, Metal-organic framework (MOF)-based drug delivery, Curr. Med. Chem. 2020;27:5949–69. https://doi.org/10.2174/0929867326666190618152518.

15. Su H, Lv S, Song H, Shi K, Zhu J, Zhang Y. Recent advances in continuous zirconium-based metal–organic framework membranes for high-precision separation, Sep. Purif. Technol. 2024;339:127318. https://doi.org/10.1016/j.seppur.2024.127318.

16. Winarta J, Shan B, McIntyre SM, Ye L, Wang C, Liu J, Mu B. A decade of UiO-66 research: a historic review of dynamic structure, synthesis mechanisms, and characterization techniques of an archetypal metal–organic framework, Cryst. Growth Des. 2019;20:1347–62. https://doi.org/10.1021/acs.cgd.9b00955.

17. Vahabi AH, Norouzi F, Sheibani E, Rahimi-Nasrabadi M, Functionalized Zr-UiO-67 metal–organic frameworks: structural landscape and application, Coord. Chem. Rev. 2021;445:214050. https://doi.org/10.1016/j.ccr.2021.214050.

18. Rego RM, Kurkuri MD, Kigga M, A comprehensive review on water remediation using UiO-66 MOFs and their derivatives, Chemosphere 2022;302: 134845. https://doi.org/10.1016/j.chemosphere.2022.134845.

19. Karimzadeh Z, Jouyban A, Ostadi A, Gharakhani A, Rahimpour E. A sensitive determination of morphine in plasma using AuNPs@UiO-66/PVA hydrogel as an advanced optical scaffold, Anal. Chim. Acta 2022;1227:340252. https://doi.org/10.1016/j.aca.2022.340252.

20. Murthy AS, Rao C. Spectroscopic studies of the hydrogen bond, Appl. Spectrosc. Rev. 1968;2: 69–191. https://doi.org/10.1080/05704926808050887.

21. Li R, Liu T, Wang K. Hyaluronic acid-modified zirconium phosphate nanoparticles for potential lung cancer therapy, Biomed. Tech. 2017;62:67–73. https://doi.org/10.1515/bmt-2015-0238.

22. Zhuang WR, Wang Y, Cui PF, Xing L, Lee J, Kim D, Jiang HL, Oh YK. Applications of π–π stacking interactions in the design of drug-delivery systems, J. Control. Release 2019;294:311–26. https://doi.org/10.1016/j.jconrel.2018.12.014.

23. Liu K, Chen W, Yang T, Wen B, Ding D, Keidar M, Tang J, Zhang W. Paclitaxel and quercetin nanoparticles co-loaded in microspheres to prolong retention time for pulmonary drug delivery, Int. J. Nanomedicine 2017;12:8239–55. https://doi.org/10.2147/IJN.S147028.

24. Lakowicz JR, Weber G, Quenching of fluorescence by oxygen: probe for structural fluctuations in macromolecules, Biochemistry 1973;12:4161–70. https://doi.org/10.1021/bi00745a020.

25. Gowda JI, Nandibewoor ST. Electrochemical behavior of paclitaxel and its determination at glassy carbon electrode, Asian J. Pharm. Sci. 2014;9:42–9. https://doi.org/10.1016/j.ajps.2013.11.007.

26. Li H, Tian L, Yang S, Li C, Song Y, Li R, Guo Y, Lu J. A signal-on electrochemiluminescence (ECL) sensor based on luminol@carbon nanotubes and CdTe–ZnS@hydroxyapatite for the detection of paclitaxel, Microchem. J. 2024;204:111102. https://doi.org/10.1016/j.microc.2024.111102.

27. Sun W, Song B, Li S. Fabrication of carbon dots–modified electrode for electrochemical sensing of paclitaxel as an important anticancer drug, Alex. Eng. J. 2024;105:682–91. https://doi.org/10.1016/j.aej.2024.08.027.

28. Jiang X, Qu A, Xu X, Kuang H, Liu L, Xu C. A gold-based multiplex immunochromatographic sensor for detecting paclitaxel, methotrexate, and 5-fluorouracil in clinical samples, Nano Res. 2024;17:6420–29. https://doi.org/10.1007/s12274-024-6649-7.

29. Bernabeu E, Flor S, Hocht C, Taira C, Chiappetta D, Tripodi V, Lucangioli S. Development and validation of a highly sensitive HPLC method for determination of paclitaxel in pharmaceutical dosage forms and biological samples, Curr. Pharm. Anal. 2014;10:185–92. https://doi.org/10.2174/1573412910666140409002944.

30. Li S, Fu Y, Zu Y, Sun R, Wang Y, Zhang L, Luo H, Gu C. T. Efferth, Determination of paclitaxel and other six taxoids in Taxus species by high-performance liquid chromatography–tandem mass spectrometry, J. Pharm. Biomed. Anal. 2009;49:81–9. https://doi.org/10.1016/j.jpba.2008.10.006.

31. Rodriguez J, Contento AM, Castaneda G, Munoz L, Berciano MA. Determination of morphine, codeine, and paclitaxel in human serum and plasma by micellar electrokinetic chromatography, J. Sep. Sci. 2012;35:2297–306. https://doi.org/10.1002/jssc.201200375.

32. Cline DJ, Zhang H, Lundell GD, Harney RL, Riaz HK, Jarrah J, Li Y, Miyazaki M, Courtney JB, Baburina I, Salamone SJ. Development and evaluation of a nanoparticle-based immunoassay for determining paclitaxel concentrations on routine clinical analyzers, Ther. Drug Monit. 2013;35:809–15. https://doi.org/10.1097/ftd.0b013e318296be01.

33. Bai J, Chen L, Zhu Y, Wang X, Wu X, Fu Y. A novel luminescence sensor based on porous molecularly imprinted polymer–ZnS quantum dots for selective recognition of paclitaxel, Colloids Surf. A 2021;610:125696. https://doi.org/10.1016/j.colsurfa.2020.125696.

34. Chao Z, Tan M, Paudel MK, Sakamoto S, Ma L, Sasaki-Tabata K, Tanaka H, Shoyama Y, Xuan L, Morimoto S. Development of an indirect competitive enzyme-linked immunosorbent assay (icELISA) using highly specific monoclonal antibody against paclitaxel, J. Nat. Med. 2013;67:512–8. https://doi.org/10.1007/s11418-012-0708-1.